Expression and Therapeutic Targeting of TROP-2 in Treatment-Resistant Prostate Cancer

Jamie M. Sperger[1,2], Kyle T. Helzer[3], Charlotte N. Stahlfeld[2], Dawei Jiang[4,5,6], Anupama Singh[2], Katherine R. Kaufmann[2], David J. Niles[7], Erika Heninger[2], Nicholas R. Rydzewski[3], Liguo Wang[8], Liewei Wang[8], Rendong Yang[9,10], Yanan Ren[10], Jonathan W. Engle[11], Peng Huang[5], Christos E. Kyriakopoulos[1,2], Susan F. Slovin[12], Howard R. Soule[13], Shuang G. Zhao[2,3], Manish Kohli[8], Scott T. Tagawa[14], Weibo Cai[2,4,11], Scott M. Dehm[9], and Joshua M. Lang[1,2]

ABSTRACT

Purpose: Men with metastatic castration-resistant prostate cancer (mCRPC) frequently develop resistance to androgen receptor signaling inhibitor (ARSI) treatment; therefore, new therapies are needed. Trophoblastic cell-surface antigen (TROP-2) is a transmembrane protein identified in prostate cancer and overexpressed in multiple malignancies. TROP-2 is a therapeutic target for antibody–drug conjugates (ADC).

Experimental Design: TROP-2 gene (*TACSTD2*) expression and markers of treatment resistance from prostate biopsies were analyzed using data from four previously curated cohorts of mCRPC ($n = 634$) and the PROMOTE study (dbGaP accession phs001141.v1.p1, $n = 88$). EPCAM or TROP-2–positive circulating tumor cells (CTC) were captured from peripheral blood for comparison of protein ($n = 15$) and gene expression signatures of treatment resistance ($n = 40$). We assessed the efficacy of TROP-2–targeting agents in a mouse xenograft model generated from prostate cancer cell lines.

Results: We demonstrated that *TACSTD2* is expressed in mCRPC from luminal and basal tumors but at lower levels in patients with neuroendocrine prostate cancer. Patients previously treated with ARSI showed no significant difference in *TACSTD2* expression, whereas patients with detectable *AR-V7* expression showed increased expression. We observed that TROP-2 can serve as a cell surface target for isolating CTCs, which may serve as a predictive biomarker for ADCs. We also demonstrated that prostate cancer cell line xenografts can be targeted specifically by labeled anti–TROP-2 agents *in vivo*.

Conclusions: These results support further studies on TROP-2 as a therapeutic and diagnostic target for mCRPC.

Introduction

Men who progress to castration-resistant prostate cancer (CRPC) have a poor prognosis owing to lethal widespread metastatic disease. In the last decade, there has been a significant increase in the number of approved treatments for men with CRPC. However, none of these therapies is curative, and there is a significant need for new agents. Many of these treatments target the androgen receptor (AR) and the AR signaling pathway (androgen receptor signaling inhibitors, ARSI); thus, the development of persistent AR activity is a common mechanism of resistance to these agents. *AR* amplifications, structural rearrangements, and mutations are the most frequent genomic alterations in CRPC after treatment with ARSIs (1–4). Expression of *AR* splice variants (AR-V), including *AR-V7* and *AR-V9*, is associated with primary resistance and reduced overall survival (OS) in patients treated with ARSIs (5–7). Given the difficulties associated with ARSI resistance, new therapeutic strategies that focus on targets outside the AR signaling axis are critically needed.

Recent advances in drug development strategies, including antibody–drug conjugates (ADC), targeted radionuclide therapy, and chimeric antigen receptor (CAR) T or NK cells, present new modalities for targeting cell surface antigens overexpressed in human cancers. Trophoblastic cell-surface antigen (TROP-2), first identified as a cell surface marker for trophoblast cells with significant homology to EPCAM, has been identified as a potential target in solid tumors (8). TROP-2 can be detected in a number of normal tissues, including epithelium of breast, liver, pancreas, prostate, salivary gland, and uterus (9), although toxicities in a randomized phase III trial in triple-negative breast cancer (TNBC) were predominantly nausea (57%), diarrhea (59%), neutropenia (63%), and rash (46%; ref. 10). However, TROP-2 is overexpressed in many human epithelial cancers, including prostate, breast, gastric, colorectal, pancreatic, cervical, urothelial, and ovarian carcinomas (11–14). This expression pattern has led to the investigation of TROP-2 as a potential target for the treatment of multiple cancers. Sacituzumab govitecan (SG) was the first FDA-approved approach to target TROP-2, but others, including

[1]Department of Medicine, University of Wisconsin–Madison, Madison, Wisconsin. [2]Carbone Cancer Center, University of Wisconsin–Madison, Madison, Wisconsin. [3]Department of Human Oncology, University of Wisconsin–Madison, Madison, Wisconsin. [4]Department of Radiology, University of Wisconsin, Madison, Wisconsin. [5]Guangdong Key Laboratory for Biomedical Measurements and Ultrasound Imaging, Laboratory of Evolutionary Theranostics, School of Biomedical Engineering, Health Science Center, Shenzhen University, Shenzhen, China. [6]Department of Nuclear Medicine, Union Hospital, Tongji Medical College, Huazhong, University of Science and Technology, Wuhan, China. [7]Department of Biomedical Engineering, University of Wisconsin–Madison, Madison, Wisconsin. [8]Mayo Clinic, Rochester, Minnesota. [9]Masonic Cancer Center and Departments of Laboratory Medicine and Pathology and Urology, University of Minnesota, Minneapolis, Minnesota. [10]The Hormel Institute, University of Minnesota, Austin, Minnesota. [11]Department of Medical Physics, University of Wisconsin, Madison, Wisconsin. [12]Memorial Sloan Kettering Cancer Center, New York, New York. [13]Department of Science, Prostate Cancer Foundation, Santa Monica, California. [14]Division of Hematology and Medical Oncology, Department of Medicine, Weill Cornell Medical College, New York.

J.M. Sperger, K.T. Helzer, and C.N. Stahlfeld contributed equally as co-authors of this article.

Corresponding Author: Joshua M. Lang, Carbone Cancer Center, University of Wisconsin-Madison, 1111 Highland Avenue, WIMR 7151, Madison, WI 53705. Phone: 608-262-0705; E-mail: jmlang@medicine.wisc.edu

Clin Cancer Res 2023;29:2324–35

doi: 10.1158/1078-0432.CCR-22-1305

Translational Relevance

Patients with castrate-resistant prostate cancer (CRPC) that has progressed to androgen receptor signaling inhibitors (ARSI) have limited options for treatment. Targeted therapies, including antibody–drug conjugates (ADC), offer new avenues for drug development. In this study, we demonstrated that TROP-2 is expressed in tumors from the majority of patients who have progressed on ARSI and that mechanisms of resistance such as AR gene amplification and expression of AR splice variants do not significantly decrease the expression of TROP-2. However, a subset of patients with neuroendocrine prostate cancer may show decreased expression of TROP-2. These results support the testing of TROP-2–targeted therapies in patients with ARSI-resistant adenocarcinoma.

datopotamab deruxtecan (Dato-Dxd), are in clinical trials. SG is an ADC that targets TROP-2 and is composed of an anti–TROP-2–humanized antibody (RS7) linked by a moderately stable carbonate bond to SN-38, a topoisomerase I inhibitor, and the active metabolite of irinotecan (15). Clinical trials with SG have demonstrated its efficacy in multiple cancer types, and SG has recently been approved for TNBC (16) and urothelial cancer (17). A second ADC, Dato-Dxd, also targets TROP-2 and is in trials for TNBC and non–small cell lung cancer (18, 19). Preclinical data have demonstrated TROP-2 expression in prostate cancer in both primary and metastatic sites, suggesting that TROP-2–targeted therapies may display significant efficacy in men with this disease (20, 21). However, in-depth analysis of TROP-2 expression in mCRPC and its effect on ARSI treatment resistance has not been performed, and its targeting efficacy is unknown.

In this report, we demonstrated that *TACSTD2* (the gene encoding TROP-2) mRNA is expressed in most patients with CRPC, and its expression is not affected by previous treatment or resistance to ARSIs. Similar to the cancer-specific cell surface marker EPCAM, TROP-2 can serve as a cell surface target to isolate circulating tumor cells (CTC) from liquid biopsies, which can be used for further molecular analyses. We also demonstrated the specificity and efficacy of targeting TROP-2 in a xenograft mouse model using prostate cancer cell lines and radiolabelled TROP-2 antibodies. These data identified TROP-2 as a potential therapeutic target for mCRPC treatment.

Materials and Methods

Interrogation of public gene expression databases

The expression of *AR-V7* and *AR-V9* in the PROMOTE database (dbGaP accession phs001141.v1.p1) was determined by calculating the number of split RNA-seq reads crossing the *AR* exon 3/CE3 (*AR-V7*) or exon 3/CE5 (*AR-V9*) splice junctions and normalizing to the total split RNA-seq reads per sample, as previously described (2). The expression levels of *TACSTD2*, *EPCAM*, *SYP*, and *CHGA* in the PROMOTE database were determined as previously described (22). RNA-seq data from 4 mCRPC cohorts Fred Hutchinson Cancer Research Center (FHCRC) autopsy cohort (23), $n = 157$; Weill Cornell Medicine (WCM) neuroendocrine prostate cancer–enriched cohort (24), $n = 49$; Stand Up 2 Cancer/Prostate Cancer Foundation (SU2C/PCF) East Coast Dream Team (ECDT) mCRPC cohort (1, 25), $n = 266$; and SU2C/PCF West Coast Dream Team (WCDT) mCRPC cohort (refs. 3, 26–28; $n = 162$) were curated and processed as previously described (29). Only previously published data were used for this study. FHCRC, WCM, and the ECDT were downloaded from www.cbioportal.org. WCDT genomics data are available from dbGaP (phs001648) and EGA (EGAD00001009065).

Cell culture

The prostate cancer cell line LAPC-4 (ATCC Cat# CRL-13009, RRID:CVCL_4744) was a gift from Dr. Douglas McNeel (University of Wisconsin-Madison) and authenticated by short tandem repeat profiling in 2014 by DDC Medical. LAPC4s were cultured in DMEM Medium (Corning) supplemented with 20% FBS (Gibco, Thermo Fisher Scientific), 1% sodium pyruvate (Corning), 0.5% beta-mercaptoethanol, and 2% penicillin–streptomycin (HyClone), in Poly-D-Lysine coated tissue culture flasks. VCAPs (ATCC Cat# CRL-2876, RRID:CVCL_2235) were cultured in DMEM supplemented with 10% FBS and 2% penicillin–streptomycin. LNCaP (ATCC Cat# CRL-1740, RRID:CVCL_1379), DU145 (ATCC Cat# HTB-81, RRID:CVCL_0105), 22Rv1 (ATCC Cat# CRL-2505, RRID:CVCL_1045), and PC3 (ATCC Cat# CRL-7934, RRID:CVCL_0035) were purchased from the ATCC and were cultured in RPMI medium (Corning) supplemented with 10% FBS, 2% penicillin–streptomycin, 1% modified non-essential amino acids (HyClone), 1% sodium pyruvate, and 0.5% beta-mercaptoethanol. LnCAP, VCAP, DU145, 22Rv1, and PC3 were authenticated in 2017 by the Wisconsin Translational Research Initiatives at the Pathology Laboratory at the University of Wisconsin.

Preparation of paramagnetic particles

Goat polyclonal antibodies to the epithelial cell adhesion molecule (R&D Systems Cat# AF960, RRID:AB_355745) and TROP-2 (R&D Systems Cat# AF650, RRID:AB_2205667) were biotinylated according to the Dynabeads FlowComp Flexi manufacturer's instructions (Thermo Fisher Scientific). Streptavidin-coupled paramagnetic particles (PMP) from the Dynabeads FlowComp Flexi kit (Thermo Fisher Scientific) were used at a concentration of 250 μg per reaction for live CTC isolation. Sera-Mag SpeedBeads blocked streptavidin PMPs were used at a concentration of 75 μg per reaction for fixed CTC isolation. The PMPs were washed twice and resuspended in 0.1% Tween-20 in PBS before the addition of biotinylated anti-EPCAM or anti–TROP-2. The PMPs and antibodies were mixed for 30 minutes at room temperature, followed by three washes and resuspension in 0.1% BSA in PBS.

Flow cytometry and cell line capture

Cells were harvested at >80% confluence using 0.25% trypsin and filtered through a 40-μm mesh filter. A total of 10^6 single cells were stained with Ghost Dye Violet 510 (Tonbo Biosciences) following anti-EPCAM-Alexa Fluor 488 (BioLegend Cat# 324210, RRID:AB_756084) and anti-TROP-2-PE (BD Biosciences Cat# 564837, RRID:AB_2738975) antibodies. Cells were acquired on a BD LSR Fortessa instrument, and data were analyzed using FlowJo v. 9.9 software (BD Biosciences, RRID:SCR_008520). The mean fluorescence intensity (MFI) was extracted from single, live cells.

To measure capture efficiency, cell lines were labeled with the vital dye Calcein AM (cat# 65–0853–39; Thermo Fisher Scientific). 250 mg of PMPs bound to the indicated antibody and 100 cells from indicated cell line were added to a mixture of 5 mmol/L EDTA, 0.001% Tween-20 and supplemented with 0.1% BSA in PBS. This mixture was tumbled for 30 minutes in a 4°C cold room to bind PMPs to cells. PMP-bound cells were captured by magnetic separation. Both the input well and captured cells were counted to determine the percentage of captured cells ($n = 3$ for all cell lines).

Clinical study design

A prospective biomarker study was performed to evaluate the expression of AR protein and splice variant expression in CTCs from patients with prostate cancer receiving or who had received systemic treatment with androgen deprivation therapy (ADT), chemotherapy, AR-targeted therapies, or Radium 223. Patients were required to have histologically confirmed prostate adenocarcinoma and documented metastases, as confirmed by CT or bone scanning with technetium-99m–labeled methylene diphosphonate. All authors vouch for the completeness and integrity of the data and for the fidelity of the study to the clinical protocol. Peripheral blood samples for CTC analysis were obtained from eligible patients at the time of disease evaluation using serum prostate-specific antigen (PSA) and radiographic imaging if PSA progression was documented. All laboratory investigators were blinded to the clinical information when determining the CTC results.

VERSA operation for clinical samples

Details of VERSA manufacturing and operation are described by Sperger and colleagues (30). Briefly, blood specimens were collected in vacutainer tubes (BD Biosciences) containing EDTA anticoagulant. Mononuclear cells were isolated using the Ficoll-Paque Plus gradient (GE Healthcare). Samples for gene expression analysis were CD45 depleted using CD45 microbeads (Miltenyi Biotec) following the manufacturer's instructions to improve the purity of live cell capture of CTCs. Samples from these patients were split, and CTCs were isolated with either EPCAM or TROP-2 antibodies using the VERSA platform, followed by mRNA extraction and gene expression analysis for a panel of genes involved in AR signaling as well as markers of NEPC. Samples for enumeration and AR protein analysis were fixed using a BD Cytofix (BD Biosciences). CTCs were isolated by VERSA using antibodies against EPCAM or TROP-2 conjugated to FlowComp PMPs, as described above. Downstream processes, including immunofluorescent staining and extraction of mRNA and DNA, are integrated into VERSA (30). qPCR was performed as previously described (31).

Immunofluorescent image analysis

CTCs were assessed by immunofluorescence staining. The following antibodies were used to identify CTCs and assess EPCAM and TROP-2 staining as indicated in the figure legends: Anti-CD45 (BioLegend Cat# 304018, RRID:AB_389336), Anti-CD34 (BioLegend Cat# 343508, RRID:AB_1877133), Anti-CD11B (BioLegend Cat# 101218, RRID:AB_389327), Anti-CD66B (BioLegend Cat# 305109, RRID:AB_2563170), Anti-Pan cytokeratin (BioLegend Cat# 628602, RRID:AB_439775 or Abcam Cat# ab49779, RRID:AB_869395), Anti-Androgen Receptor (Cell Signaling Technology Cat# 5153S, RRID:AB_10692774), Anti-EPCAM (Abcam Cat# ab112068, RRID:AB_10861805) or Anti-TROP-2 (BD Biosciences Cat# 940370, RRID:AB_2876239) and Hoechst 33342 (Thermo Fisher Scientific). Extracellular antibodies were stained at 4°C for 30 minutes. For intracellular and nuclear staining of cells (**Fig. 2**), cells were stained as described by Sperger and colleagues (30). For intracellular staining (**Fig. 4**), cells were permeabilized, stained, and washed with BD Perm/Wash. Images were taken with a 10x objective using Nikon Eclipse Ti-E with an ORCA-Flash 4.0 V2 Digital CMOS camera (Hamamatsu) and NIS-Elements AR Microscope Imaging Software (RRID:SCR_014329, Nikon Instruments). Images were background subtracted, and CTCs were determined by Hoechst-positive staining, cytokeratin^{+} and CD45^{-}/CD34^{-}/CD66b^{-}.

In vivo imaging

The detailed procedures for chelator conjugation and radiolabeling of antibodies with Cu-64 have been reported previously (32) and are outlined below. Prostate cancer cell lines (LAPC4, PC3, and 22rv1) were implanted subcutaneously into 4–6 weeks male athymic nude mice (Hsd:Athymic Nude-*Foxn1*^{nu}, Envigo, RRID:IMSR_ENV:HSD-069). Tumor sizes were monitored twice a week, and tumor-bearing mice were used for PET imaging when tumor diameters reached 8–10 mm.

PET was performed using an Inveon microPET/microCT scanner (Siemens Medical Solutions). Tumor-bearing mice injected with ^{64}Cu-NOTA-TROP-2 antibody or ^{64}Cu-NOTA-IgG (3.7–7.4 Mbq, 0.1–0.2 mCi) were anesthetized with 2% of isoflurane and placed on the scanner in prone position. Longitudinal PET scanning was performed at 4, 12, 24, and 48 hours after the intravenous administration of the radiotracers. Each scan collected 40 million coincidence events before 24 hours and 20 million at 48 hours. Images were reconstructed using the three-dimensional ordered subset expectation maximization (OSEM3D) algorithm. Region-of-interest analysis of the images was performed using the Inveon Research Workplace software (Siemens Medical Solutions), and tracer (^{64}Cu-NOTA-TROP-2 or ^{64}Cu-NOTA-IgG) uptake in different tissues was denoted as the percentage of injected dose per gram (%ID/g; mean ± SD).

Chelator conjugation

The antibody used in these studies was the same goat-polyclonal antibody used for CTC capture studies, as described previously in this article (R&D Systems Cat# AF650, RRID:AB_2205667). 1 mg of anti-TROP-2 antibody was dissolved in 1 × PBS (pH 7.2–7.4), and p-SCN-Bn-NOTA (Macrocyclics) in DMSO (10 μL) was added at a 10:1 molar ratio. The final pH of the solution was adjusted to 8.5–9.0 using sodium carbonate. The reaction mixture was maintained at room temperature for 2 hours with constant shaking. NOTA-TROP-2 antibody was purified using PD-10 columns (GE Healthcare) with 1 × PBS as the elution buffer. Non-specific IgG was used as a control antibody and was conjugated to produce NOTA-IgG. We performed radiolabeling titration after NOTA conjugation and found that the average number of chelators per antibody was approximately 2.1.

Radiolabeling of antibodies

Radiolabeling of NOTA-TROP-2 with Cu-64 was performed our previous procedure (33). Approximately 74 MBq (2 mCi) of $^{64}CuCl_2$ was added to 300 μL NaAc buffer (0.5 mol/L, pH 5.0–5.5). Following the addition of 200-μg NOTA-TROP-2 or NOTA-IgG, the solution was incubated at 37°C for 1 hour with constant shaking (500–600 rpm). ^{64}Cu-labeled antibody was purified using a PD-10 column with 1 × PBS as the elution buffer. The fractions with the highest radioactivity were used in animal studies.

Ex vivo biodistribution study

After the PET scan at the end point (48 hours), all mice were euthanized, and organs/tissues of interest were collected, wet-weighed, and counted using a gamma counter (Wizard 2, PerkinElmer). The results of biodistribution in different organs are also denoted as %ID/g (mean ± SD).

Therapy preparation and administration

Two study groups were used for the *in vivo* therapy of LAPC4 tumor-bearing mice: the IgG group and ^{90}Y-DTPA-TROP-2 group (150 μCi per mouse, approximately 50 μg of TROP-2 antibody). All mice received a single dose of the treatment agent in a total volume of

200 μL PBS via tail vein injection. From the day of injection, we monitored the body weight, tumor volume, and general appearance of all mice every other day for two weeks to assess treatment efficacy.

Prostate cancer cell lines (LAPC4, PC3, and 22RV1) were implanted subcutaneously into 4–6 weeks male athymic nude mice (Hsd:Athymic Nude-*Foxn1*^{nu}, Envigo). Tumor sizes were monitored twice a week, and tumor-bearing mice were used for PET imaging when tumor diameters reached 8–10 mm.

TROP-2 was prepared for radioimmunotherapy by conjugation with DTPA (macrocyclics) using the same method as NOTA conjugation. DTPA-TROP-2 was then subjected to $^{90}YCl_3$ labeling (PerkinElmer). A total of 74 MBq (2 mCi) of $^{90}YCl_3$ was added to 300 μL NaAc buffer (0.5 mol/L, pH 5.0–5.5). Following the addition of 300-μg DTPA-TROP-2, the solution was incubated at 37°C for 1 hour with constant shaking (500–600 rpm). ^{90}Y-labeled antibodies were purified using a PD-10 column with 1 × PBS as the elution buffer. The fractions with the highest radioactivity were used in animal studies.

Two study groups were used for the *in vivo* therapy of LAPC4 tumor-bearing mice: the IgG group and ^{90}Y-DTPA-TROP-2 group (150 μCi per mouse, approximately 50 μg of TROP-2 or control antibody). All mice received a single dose of the treatment agent in a total volume of 200-μL PBS via tail vein injection.

Monitoring of treatment efficacy and safety

From the day of injection, we monitored the body weight, tumor volume, and general appearance of all mice every other day for two weeks to assess treatment efficacy. At the end of the experiment, we measured the complete blood count of all mice to evaluate the toxicity of ^{90}Y-DTPA-TROP-2 *in vivo*.

Statistical analysis

For comparisons of *TACSTD2* expression between sample categories in the 4 mCRPC cohorts, a Wilcoxon rank-sum test or Kruskal–Wallis test was used to calculate *P* values and the specific test used is noted in each figure and figure legend (**Figs. 1** and **2**). For survival analysis, a Cox proportional hazard model was implemented on *TACSTD2* as a continuous variable using the "survival" packing in R (R v4.0.3; survival v3.2–13). For the Cox model, *TACSTD2* expression was scaled by dividing each value by the standard deviation (SD) of *TACSTD2* expression, thus a unit change of 1 represents a single SD in *TACSTD2* expression (**Fig. 1D**). Gene set enrichment analysis (GSEA) was performed using the "fgsea" package in R (fgsea v1.16.0) using all genes ranked by the Spearman correlation of their expression with *TACSTD2* expression (**Fig. 2F**). For comparison of CTCs, we used linear regression to compare CTC enumeration values and Lin's concordance correlation coefficient to compare gene expression values between EPCAM and TROP-2–captured CTCs (**Fig. 3** and Supplementary Fig. S3). For imaging studies, quantitative data were shown as mean ± SD. For tumor volume analysis in mouse experiments, the Student *t* test was used for significance test using a 95% confidence interval. For all tests, a *P* value less than 0.05 was considered statistically significant (**Fig. 5**).

Study approval

CTC collection studies were approved by the institutional review board of the University of Wisconsin (2014–1214) in accordance with the Belmont Report and U.S. Common Rule and all patients provided written informed consent. All animal experiments were performed following our laboratory protocol approved by the University of Wisconsin Institutional Animal Care and Use Committee.

Data availability statement

Data from the FHCRC, WCM, and SU2C/PCF studies are available at cBioPortal (FHCRC: www.cbioportal.org/study?id=prad_fhcrc; WCM: www.cbioportal.org/study?id=nepc_wcm_2016; SU2C/PCF: www.cbioportal.org/study?id=prad_su2c_2019). Data from the WCDT study are available from dbGaP (phs001648.v2.p1) and EGA (EGAD00001008487, EGAD00001009065). Data from the PROMOTE study are available at https://www.ncbi.nlm.nih.gov/gap/advanced_search/?TERM=phs001141. All requests for these data should be directed to these repositories or the authors of the original publications. Other data generated in this study are available upon request.

Results

TROP-2 expression in CRPC

We first investigated the expression level of *TACSTD2* in publicly available databases of mCRPC and assessed its correlation with clinical subtypes and sites of disease. Previous studies have shown that TROP-2 protein is detectable by IHC in nearly all prostate cancer biopsy samples and that TROP-2 is upregulated in metastatic prostate cancer tissue compared with localized disease (20, 21). Using RNA-seq data, we have previously curated from 634 mCRPC samples across four separate cohorts (29), we compared *TACSTD2* expression from tumors classified as adenocarcinoma or NEPC in published studies. Patients with adenocarcinoma were sub-classified as luminal or basal, and we observed that tumors from patients with adenocarcinoma (luminal or basal) had significantly higher *TACSTD2* than tumors from patients with NEPC (**Fig. 1A**; ref. 29). Interestingly, we also identified a smaller but significant increase in *TACSTD2* expression in tumors classified as luminal-like compared with that in basal-like tumors (**Fig. 1B**). We performed a Spearman correlation between *TACSTD2* and other cell surface targets identified by Lee and colleagues (34) in prostate cancer adenocarcinoma in our cohort, and all genes were positively correlated with *TACSTD2* supporting TROP-2 as a target for ADCs, CAR-T, or radioligand therapies in prostate cancer adenocarcinoma (Supplementary Fig. S1). We also analyzed *TACSTD2* expression in a cohort of patients with metastatic prostate cancer. Most patients exhibited *TACSTD2* expression regardless of biopsy site. However, analysis of *TACSTD2* expression at different sites in this metastatic cohort revealed that tumors from the primary site (prostate) had higher expression of *TACSTD2* than distant (non-lymph node) metastases ($P = 0.044$, Wilcoxon rank-sum test) and lymph node metastases ($P = 0.029$, Wilcoxon rank-sum test; **Fig. 1C**). However, primary and metastatic samples were not always from the same subjects, and there may be differences in prior treatment history, aggressiveness or patient demographics that could drive cancer heterogeneity and/or evolution. We performed survival analysis of the samples from patients diagnosed with adenocarcinoma for which survival data were available ($N = 195$). For the Cox proportional hazard model in the survival analysis, *TACSTD2* expression was scaled by dividing each value by the SD of *TACSTD2* expression, thus a unit change of 1 represents a single SD in *TACSTD2* expression. This analysis found that lower *TACSTD2* expression was correlated with lower OS (Cox proportional hazard model on continuous *TACSTD2* expression $P = 0.0118$; HR, 0.8218; 95% CI, 0.7053–0.9574; **Fig. 1D**). Overall, these data show that TROP-2 is expressed across the spectrum of mCRPC subtypes, with a lower relative expression in NEPC.

TROP-2 expression is not modulated by ARSI treatment or *AR* alterations

We next investigated whether *TACSTD2* levels were affected by resistance to ARSI treatment or the presence of AR alterations, including

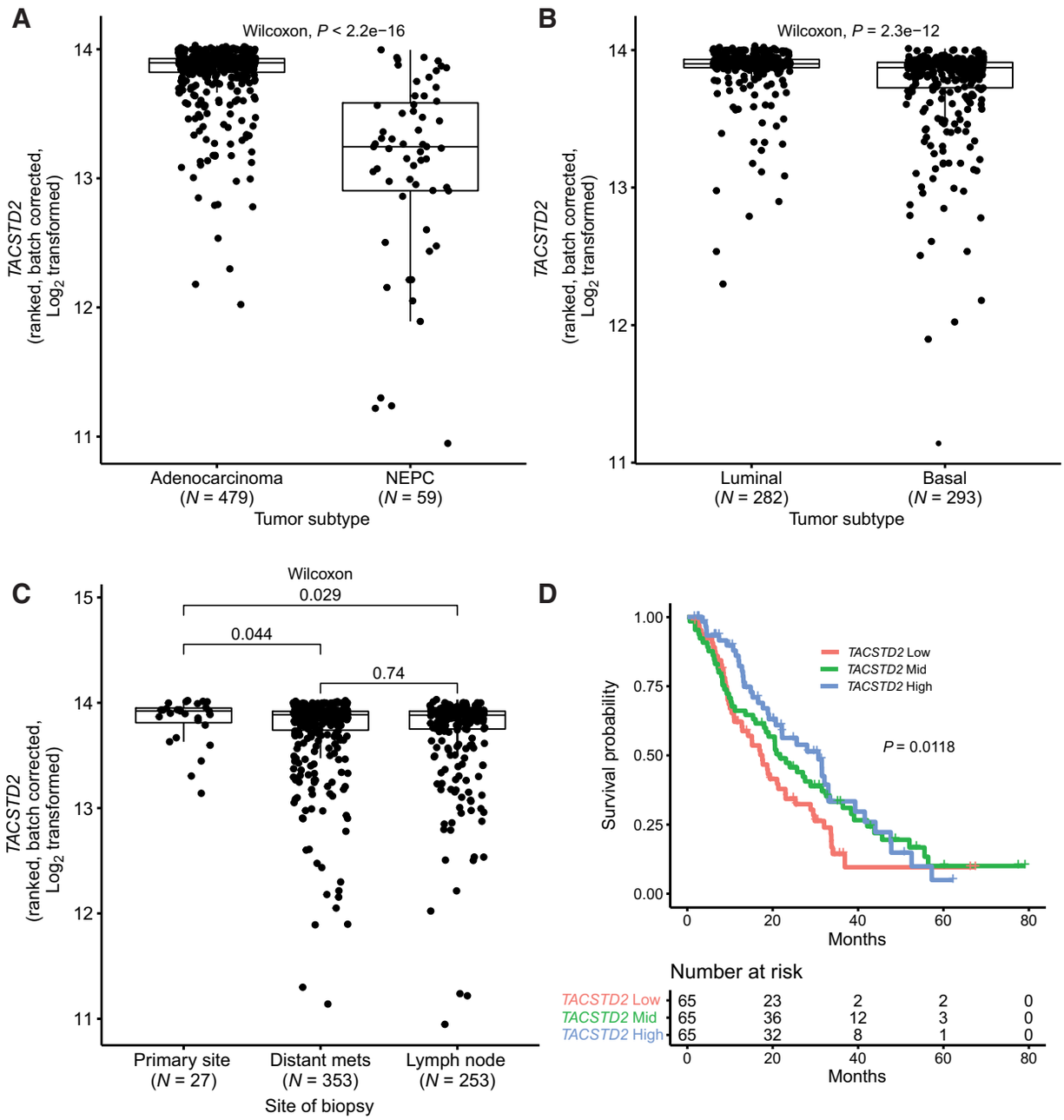

Figure 1.

TROP-2 expression in metastatic prostate cancer. *TACSTD2* expression stratified by (**A**) adenocarcinoma versus NEPC, (**B**) luminal versus basal, and (**C**) site of biopsy from patients with mCRPC ($n = 634$; normalization and batch correction of RNA-seq data described in Aggarwal et al.; ref. 29). All statistical tests performed in **A–C** are Wilcoxon rank-sum tests. (**D**) Survival analysis of *TACSTD2* high, middle, and low samples from patients with prostate adenocarcinoma. The Kaplan–Meier curve shows tertiles for visualization purposes only. Statistical testing was performed using a Cox proportional hazard model on continuous *TACSTD2* expression. For the Cox model, *TACSTD2* expression was scaled by dividing each value by the standard deviation of *TACSTD2* expression, thus a unit change of 1 represents a single standard deviation in *TACSTD2* expression (Cox proportional hazard model on continuous *TACSTD2* expression, $P = 0.0118$; HR, 0.8218; 95% CI, 0.7053–0.9574).

genomic amplifications, rearrangement, and point mutations. We assessed *TACSTD2* expression in the four published mCRPC datasets described above (29) and found no significant difference between ARSI-naïve patients and those who had previously received ARSI therapy (**Fig. 2A**; $P = 0.18$, Wilcoxon rank-sum test). To assess whether specific mechanisms of resistance to ARSI result in decreased *TACSTD2*, we first asked whether the presence of AR alterations affected *TACSTD2* expression. The four mCRPC datasets described above contained information on *AR* mutations and *AR* copy-number gains. Given the difference in *TACSTD2* expression observed between prostate adenocarcinomas

(luminal and basal) and NEPC (**Fig. 1A**), we stratified the data by these categories when comparing *TACSTD2* expression according to AR alteration status to avoid bias by subtype. We found no significant difference in *TACSTD2* expression in samples with or without an AR alteration within adenocarcinoma ($P = 0.57$, Wilcoxon rank-sum test), NEPC ($P = 0.97$, Wilcoxon rank-sum test), luminal ($P = 0.96$, Wilcoxon rank-sum test), or basal ($P = 0.18$, Wilcoxon rank-sum test), subtypes, indicating that AR mutations or copy-number gains had no effect on *TACSTD2* expression (**Fig. 2B** and **C**). The presence of AR splice variants, including *AR-V7*, in CTCs has been shown to be predictive of resistance to ARSI (5, 31, 35). The PROMOTE study assessed AR variant RNA levels in tissue biopsies and allowed us to examine the correlation between AR variants and *TACSTD2* expression (7). Interestingly, we found that when samples collected at baseline ($n = 90$) were divided into *AR-V7*–negative, *AR-V7*–low, and *AR-V7*--high tertiles, *TACSTD2* expression was highest in the group with the highest level of *AR-V7* and lowest in the *AR-V7*–negative group (**Fig. 2D**). Because we did not detect decreased expression of *TACSTD2* in *AR-V7*–positive tumors these data suggest that TROP-2 could be a viable therapeutic target in *AR-V7*–positive prostate cancers. These observations led us to investigate the pathways associated with *TACSTD2* expression. Using the data from the four CRPC datasets described above, we performed GSEA against a list of hallmark pathways and observed that the androgen response pathway was the most highly enriched pathway among *TACSTD2*-correlated genes (**Fig. 2E** and **F**). Collectively, these findings suggest that TROP-2–targeting agents may be beneficial in patients with either ARSI-sensitive or ARSI-resistant mCRPC that retain AR signaling, but may be less beneficial in patients with *de novo* or treatment-resistant neuroendocrine disease.

Capture and molecular analysis of trop-2–positive prostate cancer cells

Isolation of CTCs via liquid biopsies represents a potential source of tumor cells that could be used to assess TROP-2 expression levels to predict the efficacy of TROP-2–targeted therapies. Isolation of patient CTCs with antibodies against EPCAM has previously been shown to have prognostic relevance in CRPC and serves as a surrogate biomarker of OS (36, 37). Therefore, we assessed the feasibility of isolating CTCs using cell lines models with TROP-2 as the target antigen. We compared the efficacy of TROP-2 to EPCAM-based CTC capture.

We used the versatile exclusion-based rare sample analysis (VERSA) platform to compare the efficiency of cell line capture using anti–TROP-2 and anti-EPCAM antibodies (30). We first measured the relative levels of EPCAM and TROP-2 in six prostate cancer cell lines (22rv1, DU145, LAPC4, LNCaP, PC3, and VCaP) using flow cytometry with an Alexafluor 488–conjugated mouse mAb to EPCAM and a PE-conjugated anti-TROP-2 mouse mAb, and calculated the MFIs for each respective antigen (Supplementary Fig. S2A and S2B). Consistent with previous reports (38), we observed the highest TROP-2 surface expression in LAPC4 and DU145 cell lines and the lowest expression in LNCaP cells (Supplementary Fig. S2A and S2B). To test whether expression levels of TROP-2 correlated with single-cell capture efficiency, cell lines were isolated in parallel using VERSA with goat polyclonal antibodies against EPCAM or TROP-2 (Supplementary Fig. S2C and S2D). Capture efficiency with antibodies against TROP-2 or EPCAM was positively correlated with the expression level of the respective antigen, as measured by flow cytometry. For instance, capture efficiency was nearly 100% in the LAPC4 cell line, which displayed the highest protein levels of both EPCAM and TROP-2 (Supplementary Fig. S2C and S2D).

After confirming that the goat polyclonal antibody to TROP-2 was suitable for CTC capture in cell lines, we evaluated the isolation of CTCs with anti–TROP-2 antibodies from patients with mCRPC. We performed enumeration and immunofluorescence staining of CTCs isolated with either EPCAM or TROP-2 antibodies from matched peripheral blood specimens from 15 patients with mCRPC. Representative immunofluorescent images of isolated CTCs with either EPCAM or TROP-2 antibody capture of cells show co-expression of AR (**Fig. 3A** and **B**). Notably, the number of CTCs captured using anti-EPCAM was strongly correlated with those captured using anti–TROP-2 (Pearson $r = 0.92$; **Fig. 3C**). The patient and cell line data demonstrate that this anti–TROP-2 antibody can be used to capture prostate CTCs for molecular analysis. In addition to enumeration, we evaluated the gene expression patterns in CTC populations captured from 40 patients with mCRPC using EPCAM or TROP-2 antibodies. We found similar gene expression patterns in EPCAM and TROP-2–captured CTCs (**Fig. 3D**). We tested the correlation of gene expression values for each gene from TROP-2 captured CTCs compared with the gold standard EPCAM captured CTCs. TROP-2–captured CTCs showed similar expression of the genes in the panel to EPCAM-captured genes (Lin's concordance = 0.86; 95% CI, 0.83–0.88), though there is some heterogeneity (Supplementary Fig. S3). Overall, these data demonstrate that TROP-2 can be used as a target for CTC capture. This suggests that TROP-2–positive CTCs can be used to monitor enumeration and gene expression during treatment.

Case study of intra-patient cellular heterogeneity of trop-2 in CTCs from a patient with NEPC

The above data from prostate cancer CTCs demonstrated that the majority of patients with CRPC had TROP-2–positive CTCs. However, we would like to highlight one patient in which we observed that EPCAM- and TROP-2–captured CTCs were phenotypically distinct and corresponded to NEPC and adenocarcinoma populations as described previously in the RNA-seq studies above. At the time of the blood draw, the patient was being treated with ADT with slowly increasing serum PSA levels. This patient developed new symptoms of disease progression, and restaging scans identified progressive disease with new bone, lymph node, liver, and lung metastases. A liver biopsy was performed, which showed small-cell carcinoma of prostate origin with expression of synaptophysin (*SYP*) and chromogranin A (*CHGA*). CTCs were isolated using antibodies against EPCAM or TROP-2 as described above, and these CTCs were also stained for the expression of EPCAM and TROP-2 proteins on the surface of the cells (**Fig. 4A**). More CTCs were captured with EPCAM antibodies (606 CTCs) than with TROP-2 antibodies (380 CTCs). In CTCs captured with anti-EPCAM, we identified a distinct population of cells characterized by very high EPCAM expression (>1,000 MFI) that was not present in TROP-2–captured CTCs. The median EPCAM MFI was 2510 in the EPCAM-captured specimen and 179 in the matched TROP-2 captured specimen ($P < 0.0001$; **Fig. 4B**). The gene expression signatures of EPCAM-captured and TROP-2–captured CTCs from this patient were markedly different, further suggesting two distinct cell populations corresponding to adenocarcinoma and NEPC (**Fig. 4C**). TROP-2 CTCs displayed a pattern of gene expression consistent with a predominance of prostate adenocarcinoma, including expression of genes downstream of AR, including *TMPRSS2*, *KLK2*, *KLK3*, and *HOXB13*, whereas EPCAM-captured cells were positive for *NKX3–1* suggesting prostate origin, but with a predominantly NEPC signature evidenced by high *SYP* and *CHGA* and low levels of *AR* and downstream targets. The observation that

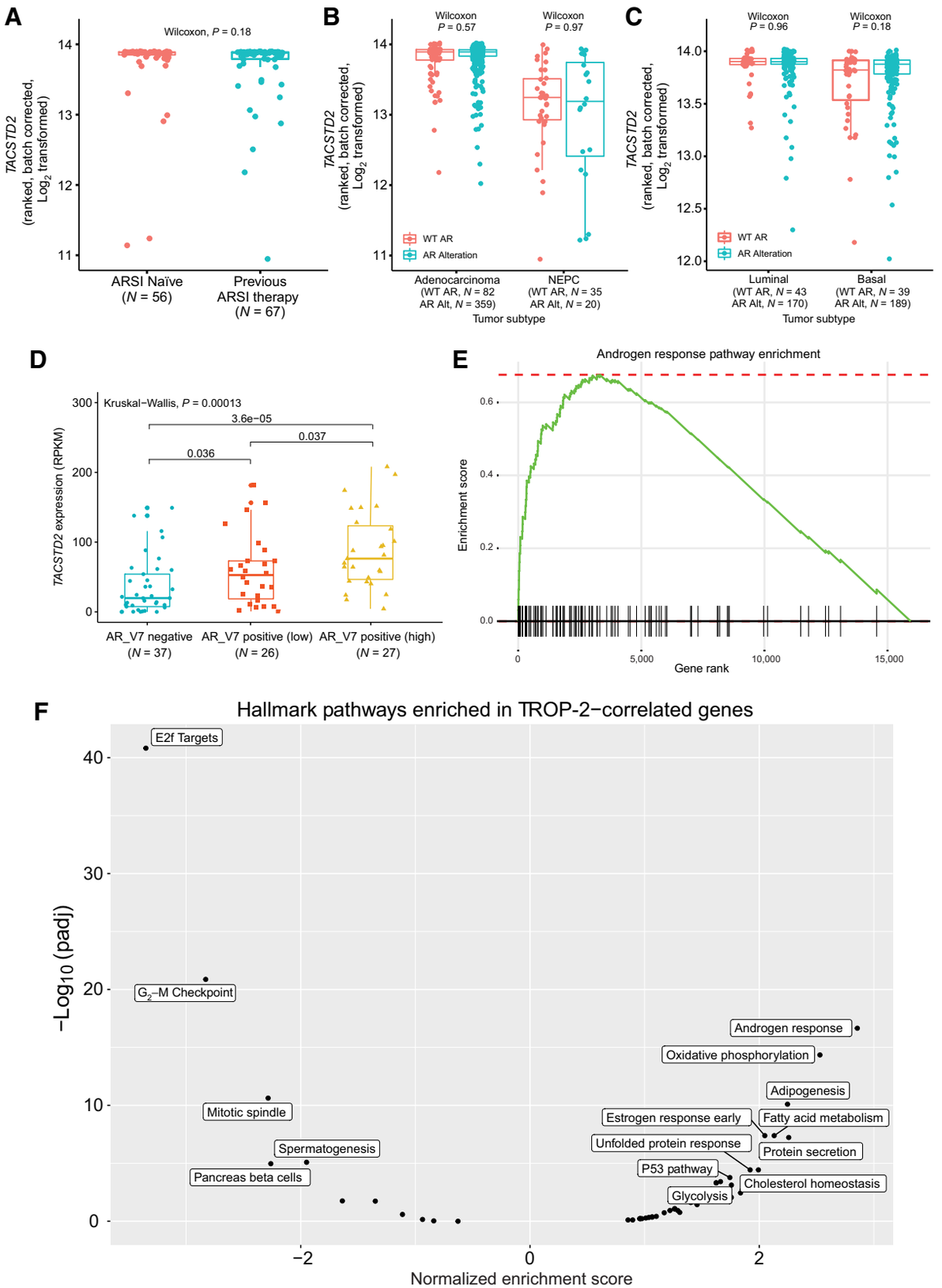
A
Wilcoxon, P = 0.18
TACSTD2 (ranked, batch corrected, Log2 transformed)
ARSI Naïve (N = 56)
Previous ARSI therapy (N = 67)
B
Wilcoxon P = 0.57
Wilcoxon P = 0.97
WT AR
AR Alteration
Adenocarcinoma (WT AR, N = 82 AR Alt, N = 359)
NEPC (WT AR, N = 35 AR Alt, N = 20)
Tumor subtype
C
Wilcoxon P = 0.96
Wilcoxon P = 0.18
Luminal (WT AR, N = 43 AR Alt, N = 170)
Basal (WT AR, N = 39 AR Alt, N = 189)
D
Kruskal–Wallis, P = 0.00013
3.6e–05
0.037
0.036
TACSTD2 expression (RPKM)
AR_V7 negative (N = 37)
AR_V7 positive (low) (N = 26)
AR_V7 positive (high) (N = 27)
E
Androgen response pathway enrichment
Enrichment score
Gene rank
F
Hallmark pathways enriched in TROP-2–correlated genes
E2f Targets
G2–M Checkpoint
Mitotic spindle
Spermatogenesis
Pancreas beta cells
Androgen response
Oxidative phosphorylation
Adipogenesis
Estrogen response early
Fatty acid metabolism
Unfolded protein response
Protein secretion
P53 pathway
Cholesterol homeostasis
Glycolysis
−Log10 (padj)
Normalized enrichment score

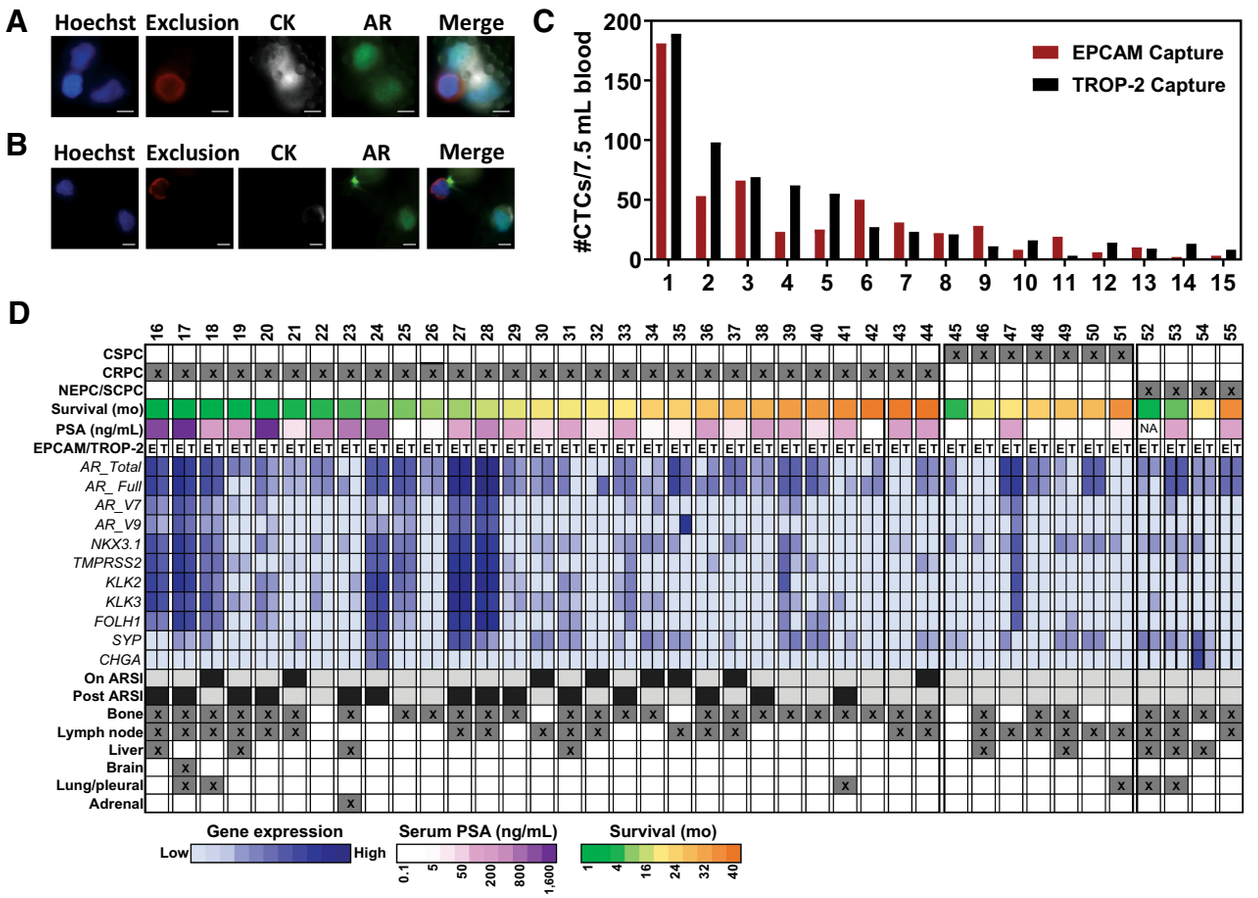

Figure 3.

Analysis of TROP-2 Captured CTCs. CTCs were captured from patients with metastatic prostate cancer using the indicated antibody. Images of representative CTCs are shown for CTCs captured using antibodies to (**A**) EPCAM and (**B**) TROP-2. CTCs are stained with Hoechst (Blue), AR (Green), CD45/CD11B/CD14 (Exclusion, Red) and Pan-Cytokeratin (CK, White; scale bars, 5 μm). (**C**) Enumeration of CTCs from 15 patients with metastatic prostate cancer captured by the indicated antibody is shown. (**D**) Gene expression analysis of EPCAM-captured and TROP-2-captured (T) CTCs from 40 patients with prostate cancer.

we captured EPCAM-positive CTCs with an NEPC-like phenotype and TROP-2–positive CTCs with an adenocarcinoma phenotype within a single patient is consistent with the hypothesis that NEPC tumor cells may express less TROP-2 than prostate cancer cells with an adenocarcinoma origin. Prospective clinical trials are needed to assess whether low or absent TROP-2 may predict resistance to TROP-2–targeted ADC.

TROP-2 as a target for molecular imaging and targeted therapy in metastatic prostate cancer

Given the expression of TROP-2 in mCRPC, regardless of prior ARSI treatment, we hypothesized that TROP-2 could serve as an imaging target for mCRPC tumor cells. We tested this hypothesis using a xenograft model to identify target TROP-2–positive tumor cells for molecular imaging and therapeutic targeting, using the same TROP-2 antibody used for CTC capture. To test this hypothesis, we generated subcutaneous mouse xenografts with cell lines expressing high levels of TROP-2 (LAPC4) and low levels of TROP-2 (PC3, 22rv1). We analyzed the targeting efficiency of ^{64}Cu-labeled anti–TROP-2 antibody (**Fig. 5A**). PET imaging showed accumulation of ^{64}Cu-anti–TROP-2 in the tumor compared with that in the IgG control ($n = 3$ for each group). In contrast, the blood pool and liver displayed a high initial activity, followed by a steady decline (**Fig. 5B**). The highest accumulation of ^{64}Cu-anti–TROP-2 was observed in the LAPC4 xenograft, which expressed the highest level of TROP-2 (**Fig. 5B**). An *ex vivo* biodistribution study confirmed tumor accumulation of the

Figure 2.

Effect of ARSI Treatment and AR Alterations on TROP-2 Expression. **A,** *TACSTD2* expression in patients from the 4 mCRPC studies stratified by ARSI naïve or previous ARSI therapy. **B,** *TACSTD2* expression in tumor biopsies from patients with and without *AR* alterations (defined as *AR* mutation or *AR* copy number amplification) from the 4 mCRPC cohorts stratified by adenocarcinoma and NEPC. **C,** *TACSTD2* expression in tumor biopsies with or without AR alteration as in (**B**), but stratified by luminal and basal mCRPC. Statistical tests performed in **A–C** are Wilcoxon rank sum tests. **D,** *TACSTD2* expression in baseline ($N = 92$) samples from the PROMOTE study divided into tertiles by expression level of *AR-V7* (Negative $n = 37$, low $n = 26$, high $n = 27$). **E,** Enrichment plot of the Androgen Response Pathway from the GSEA analysis performed in (**F**). **F,** GSEA analysis of hallmark pathways enriched in *TACSTD2*-correlated genes. A positive normalized enrichment score denotes positive correlation with *TACSTD2* expression.

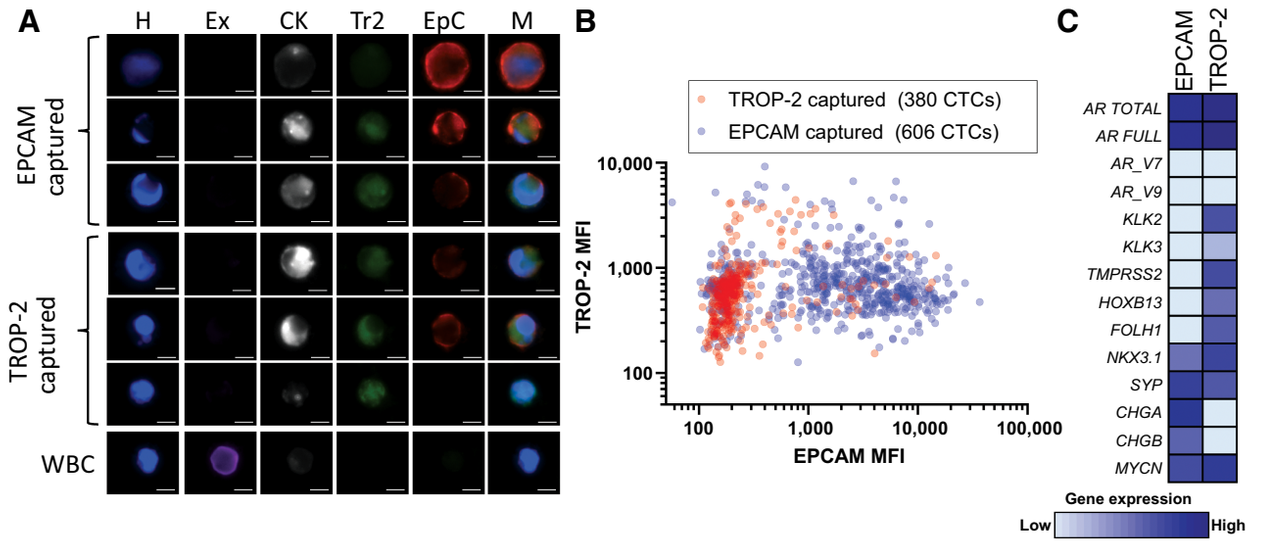

Figure 4.

CTCs are heterogeneous with respect to EPCAM and TROP-2 expression in a patient with NEPC. (**A**) CTCs were captured with EPCAM and TROP-2 antibodies in parallel and were identified positive for Hoechst (H) and pan-cytokeratin (CK) and negative for exclusion marker cocktail (Ex). Cells were also stained for EPCAM (EpC) and TROP-2 (Tr2); scale bar, 5 µm. (**B**) The mean fluorescent intensities (MFI) of TROP-2 versus EPCAM were graphed for each CTC identified after capture with antibodies to either TROP-2 (red) or EPCAM (blue) and plotted as individual cells. (**C**) Gene expression analysis of EPCAM captured and TROP-2–captured populations of cells shows expression of neuroendocrine genes and genes downstream of AR.

antibody visualized using immunoPET imaging and further suggested that TROP-2 might be a viable target for drug development in prostate cancer (Supplementary Fig. S4).

To evaluate the potential of TROP-2 as a target for mCRPC therapy, we labeled TROP-2 antibody with the radioisotope ^{90}Y to determine whether TROP-2 could direct radiotherapy to the tumor site. LAPC4 xenografts were grown for two weeks and randomized to treatment with ^{90}Y-anti–TROP-2 or IgG control ($n = 3$ for each group). The mice treated with ^{90}Y-labeled anti–TROP-2 antibody showed a significant decrease in tumor growth compared with IgG controls (**Fig. 5C**). A statistical difference can be seen at and the endpoint of 12 days after treatment ($P = 0.018$). In addition, hematoxylin and eosin staining of tumors showed tumor damage in the ^{90}Y-TROP-2 antibody–treated group compared with that in the PBS control group (**Fig. 5D**). These data demonstrate that TROP-2 can serve as a target for both molecular imaging of CRPC tumors and targeted therapies.

Discussion

mCRPC represents the end-stage of prostate cancer, where approved therapies prolong the median OS by only 2–4 months (39–43). Resistance to ARSIs, the backbone of systemic therapy for this disease, is widespread. Therefore, new therapies for the treatment of mCRPC are required. TROP-2 has emerged as a promising target outside the AR signaling axis and has been successfully used as a drug target in other malignancies (10, 16, 17, 44–46). However, its effectiveness as a target for mCRPC remains unknown. In this report, we demonstrated the feasibility of using TROP-2 as a target for mCRPC therapies and its utility for isolating CTCs to monitor the response in patients with mCRPC. We found that TROP-2 was expressed in the majority of mCRPC cases. Although expression is lower in the more aggressive NEPC subtype, there is a wide range, with some tumors still demonstrating retained expression. In addition, prior ARSI treatment or the presence of AR-modulating mutations did not significantly affect the expression of *TACSTD2*, and AR-V7 positivity may be associated with greater expression of *TACSTD2*, suggesting that agents targeting TROP-2 would be minimally affected by ARSI resistance status. Finally, mouse xenograft models demonstrated that labeled TROP-2 antibody specifically targets mCRPC tumors and that conjugating TROP-2 to a radioisotope is effective at decreasing tumor burden. These results demonstrate that targeting TROP-2 is a feasible strategy for the treatment of mCRPC and warrants further analysis in clinical trials.

ADCs, including SG and Dato-Dxd, were developed to target TROP-2. Both drugs are composed of an anti–TROP-2 antibody linked to a topoisomerase I inhibitor, which induces double-stranded DNA breaks, leading to apoptosis. Clinical trials have demonstrated the efficacy of SG in TNBC and urothelial cancer, which led to the approval of SG for these two cancer types (16, 17). A Phase I/II multicenter, single-arm basket trial (NCT01631552) evaluated the efficacy of SG in patients with advanced epithelial cancers, including prostate cancer (10). The ORR varies across different cancer types. In patients with prostate cancer, there was evidence of a clinical response in a small cohort consisting of patients with heavily pretreated disease and some patients with NEPC ($n = 11$). One patient had a complete response, and the trial demonstrated a clinical benefit rate of 27.3% in patients with prostate cancer. However, more patients are needed to assess the efficacy in prostate cancer and to target this therapy in patients most likely to respond. Our observation that TROP-2 is expressed in patients with mCRPC before and after treatment with AR-targeted therapies suggests that TROP-2–targeted therapies may be beneficial to patients whose disease develops resistance to second-generation AR-targeted therapy and serve as a target for future drug development. Interestingly, we found a positive correlation between *TACSTD2* expression and the expression *AR-V7*, indicating that patients with mCRPC who have progressed on ARSI treatment via this mechanism might benefit from agents targeting TROP-2. To address these hypotheses, we began a phase II clinical trial (NCT03725761) to assess the effectiveness of

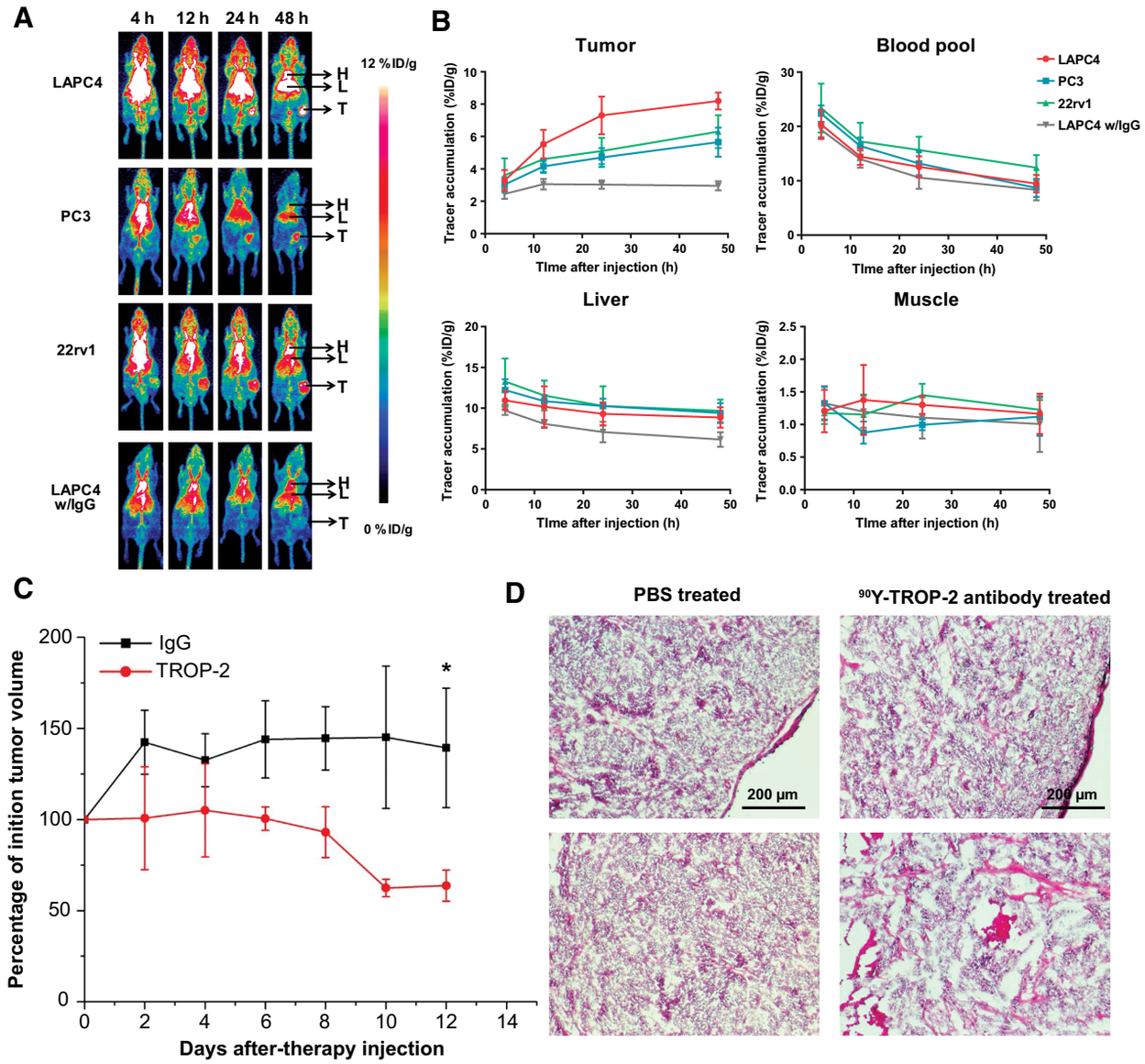

Figure 5.

TROP-2 is an Effective Target for PET imaging and treatment of xenograft mCRPC tumors. (**A**) Serial PET imaging and ROI quantifications of TROP-2 in LAPC4, PC3, and 22rv1 tumor-bearing mice injected with ^{64}Cu-labeled anti–TROP-2 antibody or non-specific IgG control as indicated at 4, 24, and 48 hours after injection. H-Heart, L-Liver, and T-Tumor. (**B**) Time–activity curves of the tumor, liver, blood, and muscle upon intravenous injection of ^{64}Cu-labeled anti–TROP-2 antibody into LAPC4, PC3 or 22rv1 tumor-bearing mice ($n = 3$). (**C**) Treatment of LAPC4 xenograft tumors with ^{90}Y-labeled TROP-2 or IgG. Tumor growth is measured as the percentage of initial tumor volume ($n = 3$). The primary endpoint of the study was pre-specified at 12 days, when all mice were sacrificed, and the time at which we would expect maximal treatment effect. Statistical inference was performed at the primary endpoint, where a Student t test was performed. *, $p < 0.05$ and was considered statistically significant. (**D**) H&E staining shows increased cell death in ^{90}Y-labeled TROP-2 sample compared with the control PBS treatment.

SG in patients with mCRPC who have progressed on abiraterone or enzalutamide.

Although SG has shown clinical benefits for patients with various malignancies, not all patients respond to treatment, and resistance has been reported (16, 46, 47). The identification and analysis of predictors of response have been challenging because of the difficulty in obtaining metastatic biopsies. The capture of CTCs represents a source of biological material that can inform the status of the tumor through minimally invasive liquid biopsy. Enumeration and gene expression analysis of these rare CTCs are prognostic when captured with EPCAM (31, 48), and our results suggest that we can also capture TROP-2–positive CTCs using a similar approach. Molecular analysis of TROP-2–positive CTCs could provide a potential companion biomarker for the evaluation of TROP-2 ADC clinical trials in prostate cancer. We hypothesized that TROP-2 positivity and protein expression may correlate with response and resistance. A liquid biomarker for TROP-2 may identify patients most likely to benefit from TROP-2–targeted therapies and help guide future clinical trials. Indeed, this is

being tested prospectively in a phase II clinical trial with SG (NCT03725761) in patients with mCRPC who have progressed on abiraterone or enzalutamide.

Authors' Disclosures

K.T. Helzer reports that their spouse is an employee of Epic Systems. S.G. Zhao reports unrelated patents licensed to Veracyte, and that a family member is an employee of Artera and holds stock in Exact Sciences. S.T. Tagawa reports grants from Gilead and Prostate Cancer Foundation during the conduct of the study; and grants and personal fees from Gilead, personal fees from Daiichi Sankyo, and grants and personal fees from Sanofi, Pfizer, Novartis, Janssen, Bayer, Seagen, and Merck outside the submitted work; in addition, S.T. Tagawa reports a patent for Gilead issued to Immunomedics/Gilead/Cornell University. W. Cai reports grants and personal fees from Focus-X Therapeutics Inc. outside the submitted work. S.M. Dehm reports grants from Prostate Cancer Foundation, US National Cancer Institute, and US Department of Defense Prostate Cancer Research Program during the conduct of the study; and personal fees from Bristol Myers Squibb/Celgene and Oncternal Therapeutics, grants from Pfizer/Astellas/Medivation, and personal fees from Janssen R&D, LLC outside the submitted work; as well as reports a patent for Androgen receptor variant inhibitors and methods of using issued. J.M. Lang reports grants from National Cancer Institute, Prostate Cancer Foundation, and Department of Defense during the conduct of the study; other support from Janssen, Astellas, Arvinas, Gilead, Sanofi, Pfizer, 4D Pharma, AstraZeneca, and Salus Discovery, LLC outside the submitted work; as well as reports a patent for CTC technology licensed to Salus Discovery, LLC. No disclosures were reported by the other authors.

Authors' Contributions

J.M. Sperger: Conceptualization, data curation, formal analysis, investigation, visualization, methodology, writing–original draft, project administration, writing–review and editing. **K.T. Helzer:** Conceptualization, data curation, formal analysis, investigation, visualization, methodology, writing–original draft, writing–review and editing. **C.N. Stahlfeld:** Conceptualization, data curation, formal analysis, investigation, visualization, methodology, writing–original draft, writing–review and editing. **D. Jiang:** Conceptualization, formal analysis, investigation, visualization, methodology, writing–original draft, writing–review and editing. **A. Singh:** Investigation, methodology, writing–review and editing. **K.R. Kaufmann:** Investigation, writing–review and editing. **D.J. Niles:** Software, formal analysis, investigation, visualization, writing–review and editing. **E. Heninger:** Conceptualization, software, formal analysis, investigation, visualization, writing–review and editing. **N.R. Rydzewski:** Conceptualization, data curation, formal analysis, investigation, visualization, methodology, writing–review and editing. **L. Wang:** Data curation, formal analysis, investigation, visualization, methodology, writing–review and editing. **L. Wang:** Data curation, formal analysis, investigation, writing–review and editing. **R. Yang:** Data curation, formal analysis, investigation, writing–review and editing. **Y. Ren:** Data curation, formal analysis, investigation, writing–review and editing. **J.W. Engle:** Resources, supervision, writing–review and editing. **P. Huang:** Supervision, writing–review and editing. **C.E. Kyriakopoulos:** Resources, investigation, writing–review and editing. **S.F. Slovin:** Resources, investigation, writing–review and editing. **H.R. Soule:** Conceptualization, funding acquisition, methodology, writing–review and editing. **S.G. Zhao:** Conceptualization, data curation, formal analysis, supervision, investigation, writing–original draft, writing–review and editing. **M. Kohli:** Resources, supervision, investigation, writing–review and editing. **S.T. Tagawa:** Conceptualization, resources, writing–review and editing. **W. Cai:** Conceptualization, supervision, investigation, writing–review and editing. **S.M. Dehm:** Conceptualization, resources, data curation, formal analysis, supervision, funding acquisition, investigation, writing–original draft, writing–review and editing. **J.M. Lang:** Conceptualization, resources, formal analysis, supervision, funding acquisition, investigation, methodology, writing–original draft, project administration, writing–review and editing.

Acknowledgments

We would like to thank all the patients who participated in this study. This work was supported by the Prostate Cancer Foundation Challenge Award 17CHAL05, NIH grant R01CA181648, DOD PCRP Grant # W81XWH-15–1-0500 (to J.M. Sperger), DOD PCRP grant W81XWH-15–1-0501 and NCI grant R01CA174777 (to S.M. Dehm), UG3 award UG3CA260692 (to J.M. Lang) and NIH Grant R01CA21209 (to M. Kohli).We are also grateful for the help of Katie Kovacich for project management and the UWCCC GU clinical research group, particularly Jamie Wiepz, Emily Nordin, Kelly Bush, and Mary Jane Staab. The authors acknowledge Menggang Yu for statistical consultation. The authors also thank the University of Wisconsin Translational Research Initiatives in Pathology Laboratory Flow Cytometry Laboratory and the Small Animal Imaging and Radiotherapy Facility, funded by the NIH UWCCC core grant P30 CA014520 for the use of their facilities and services. The BD LSR Fortessa instrument was supported by NIH Special BD LSR Fortessa grant#1S10OD018202–01.

The publication costs of this article were defrayed in part by the payment of publication fees. Therefore, and solely to indicate this fact, this article is hereby marked "advertisement" in accordance with 18 USC section 1734.

Note

Supplementary data for this article are available at Clinical Cancer Research Online (http://clincancerres.aacrjournals.org/).

Received April 28, 2022; revised July 29, 2022; accepted March 14, 2023; published first March 20, 2023.

References

1. Robinson D, Van Allen EM, Wu YM, Schultz N, Lonigro RJ, Mosquera JM, et al. Integrative clinical genomics of advanced prostate cancer. Cell 2015;161:1215–28.
2. Henzler C, Li Y, Yang R, McBride T, Ho Y, Sprenger C, et al. Truncation and constitutive activation of the androgen receptor by diverse genomic rearrangements in prostate cancer. Nat Commun 2016;7:13668.
3. Quigley DA, Dang HX, Zhao SG, Lloyd P, Aggarwal R, Alumkal JJ, et al. Genomic hallmarks and structural variation in metastatic prostate cancer. Cell 2018;174:758–69.
4. Li Y, Yang R, Henzler CM, Ho Y, Passow C, Auch B, et al. Diverse AR gene rearrangements mediate resistance to androgen receptor inhibitors in metastatic prostate cancer. Clin Cancer Res 2020;26:1965–76.
5. Antonarakis ES, Lu C, Wang H, Luber B, Nakazawa M, Roeser JC, et al. AR-V7 and resistance to enzalutamide and abiraterone in prostate cancer. N Engl J Med 2014;371:1028–38.
6. Scher HI, Lu D, Schreiber NA, Louw J, Graf RP, Vargas HA, et al. Association of AR-V7 on circulating tumor cells as a treatment-specific biomarker with outcomes and survival in castration-resistant prostate cancer. JAMA Oncol 2016;2:1441–9.
7. Kohli M, Ho Y, Hillman DW, Van Etten JL, Henzler C, Yang R, et al. Androgen receptor variant AR-V9 is coexpressed with AR-V7 in prostate cancer metastases and predicts abiraterone resistance. Clin Cancer Res 2017;23:4704–15.
8. Lipinski M, Parks DR, Rouse RV, Herzenberg LA. Human trophoblast cell-surface antigens defined by monoclonal antibodies. Proc Natl Acad Sci U S A 1981;78:5147–50.
9. Stepan LP, Trueblood ES, Hale K, Babcook J, Borges L, Sutherland CL. Expression of Trop2 cell surface glycoprotein in normal and tumor tissues: potential implications as a cancer therapeutic target. J Histochem Cytochem 2011;59:701–10.
10. Bardia A, Messersmith WA, Kio EA, Berlin JD, Vahdat L, Masters GA, et al. Sacituzumab govitecan, a Trop-2-directed antibody–drug conjugate, for patients with epithelial cancer: final safety and efficacy results from the phase I/II IMMU-132–01 basket trial. Ann Oncol 2021;32:746–56.
11. Cardillo TM, Govindan SV, Sharkey RM, Trisal P, Goldenberg DM. Humanized anti-Trop-2 IgG-SN-38 conjugate for effective treatment of diverse epithelial cancers: preclinical studies in human cancer xenograft models and monkeys. Clin Cancer Res 2011;17:3157–69.
12. Stein R, Basu A, Goldenberg DM, Lloyd KO, Mattes MJ. Characterization of cluster 13: the epithelial/carcinoma antigen recognized by MAb RS7. Int J Cancer Suppl 1994;8:98–102.
13. Cubas R, Li M, Chen C, Yao Q. Trop2: a possible therapeutic target for late stage epithelial carcinomas. Biochim Biophys Acta 2009;1796:309–14.
14. Trerotola M, Cantanelli P, Guerra E, Tripaldi R, Aloisi AL, Bonasera V, et al. Upregulation of Trop-2 quantitatively stimulates human cancer growth. Oncogene 2013;32:222–33.

15. Goldenberg DM, Cardillo TM, Govindan SV, Rossi EA, Sharkey RM. Trop-2 is a novel target for solid cancer therapy with sacituzumab govitecan (IMMU-132), an antibody–drug conjugate (ADC). Oncotarget 2015;6:22496–512.
16. Bardia A, Hurvitz SA, Tolaney SM, Loirat D, Punie K, Oliveira M, et al. Sacituzumab govitecan in metastatic triple-negative breast cancer. N Engl J Med 2021;384:1529–41.
17. Tagawa ST, Balar AV, Petrylak DP, Kalebasty AR, Loriot Y, Fléchon A, et al. TROPHY-U-01: a Phase II open-label study of sacituzumab govitecan in patients with metastatic urothelial carcinoma progressing after platinum-based chemotherapy and checkpoint inhibitors. J Clin Oncol 2021;39:2474–85.
18. Very compelling" results for ADC in TNBC trial. Cancer Discov 2022;12:280–1.
19. TROP2 ADC Intrigues in NSCLC. Cancer Discov 2021;11:OF5.
20. Trerotola M, Ganguly KK, Fazli L, Fedele C, Lu H, Dutta A, et al. Trop-2 is upregulated in invasive prostate cancer and displaces FAK from focal contacts. Oncotarget 2015;6:14318–28.
21. Trerotola M, Jernigan DL, Liu Q, Siddiqui J, Fatatis A, Languino LR. Trop-2 promotes prostate cancer metastasis by modulating beta(1) integrin functions. Cancer Res 2013;73:3155–67.
22. Wang L, Dehm SM, Hillman DW, Sicotte H, Tan W, Gormley M, et al. A prospective genome-wide study of prostate cancer metastases reveals association of wnt pathway activation and increased cell-cycle proliferation with primary resistance to abiraterone acetate-prednisone. Ann Oncol 2018;29:352–60.
23. Kumar A, Coleman I, Morrissey C, Zhang X, True LD, Gulati R, et al. Substantial interindividual and limited intraindividual genomic diversity among tumors from men with metastatic prostate cancer. Nat Med 2016;22:369–78.
24. Beltran H, Prandi D, Mosquera JM, Benelli M, Puca L, Cyrta J, et al. Divergent clonal evolution of castration-resistant neuroendocrine prostate cancer. Nat Med 2016;22:298–305.
25. Abida W, Cyrta J, Heller G, Prandi D, Armenia J, Coleman I, et al. Genomic correlates of clinical outcome in advanced prostate cancer. Proc Natl Acad Sci U S A 2019;116:11428–36.
26. Aggarwal R, Beer TM, Gleave M, Stuart JM, Rettig M, Evans CP, et al. Targeting adaptive pathways in metastatic treatment-resistant prostate cancer: update on the stand up 2 cancer/prostate cancer foundation-supported west coast prostate cancer dream team. Eur Urol Focus 2016;2:469–71.
27. Zhao SG, Chen WS, Li H, Foye A, Zhang M, Sjöström M, et al. The DNA methylation landscape of advanced prostate cancer. Nat Genet 2020;52:778–89.
28. Chen WS, Aggarwal R, Zhang L, Zhao SG, Thomas GV, Beer TM, et al. Genomic drivers of poor prognosis and enzalutamide resistance in metastatic castration-resistant prostate cancer. Eur Urol 2019;76:562–71.
29. Aggarwal R, Rydzewski NR, Zhang L, Foye A, Kim W, Helzer KT, et al. Prognosis associated with luminal and basal subtypes of metastatic prostate cancer. JAMA Oncol 2021;7:1644–52.
30. Sperger JM, Strotman LN, Welsh A, Casavant BP, Chalmers Z, Horn S, et al. Integrated analysis of multiple biomarkers from circulating tumor cells enabled by exclusion-based analyte isolation. Clin Cancer Res 2017;23:746–56.
31. Sperger JM, Emamekhoo H, McKay RR, Stahlfeld CN, Singh A, Chen XE, et al. Prospective evaluation of clinical outcomes using a multiplex liquid biopsy targeting diverse resistance mechanisms in metastatic prostate cancer. J Clin Oncol 2021;39:2926–37.
32. Yang Y, Hernandez R, Rao J, Yin L, Qu Y, Wu J, et al. Targeting CD146 with a 64Cu-labeled antibody enables *in vivo* immunoPET imaging of high-grade gliomas. Proc Natl Acad Sci U S A 2015;112:E6525–34.
33. Jiang D, Im HJ, Sun H, Valdovinos HF, England CG, Ehlerding EB, et al. Radiolabeled pertuzumab for imaging of human epidermal growth factor receptor 2 expression in ovarian cancer. Eur J Nucl Med Mol Imaging 2017; 44:1296–305.
34. Lee JK, Bangayan NJ, Chai T, Smith BA, Pariva TE, Yun S, et al. Systemic surfaceome profiling identifies target antigens for immune-based therapy in subtypes of advanced prostate cancer. Proc Natl Acad Sci U S A 2018;115: E4473–e82.
35. Armstrong AJ, Halabi S, Luo J, Nanus DM, Giannakakou P, Szmulewitz RZ, et al. Prospective multicenter validation of androgen receptor splice variant 7 and hormone therapy resistance in high-risk castration-resistant prostate cancer: the PROPHECY study. J Clin Oncol 2019;37:1120–9.
36. de Bono JS, Scher HI, Montgomery RB, Parker C, Miller MC, Tissing H, et al. Circulating tumor cells predict survival benefit from treatment in metastatic castration-resistant prostate cancer. Clin Cancer Res 2008;14: 6302–9.
37. Scher HI, Heller G, Molina A, Kheoh TS, Attard G, Moreira J, et al. Evaluation of circulating tumor cell (CTC) enumeration as an efficacy response biomarker of overall survival (OS) in metastatic castration-resistant prostate cancer (mCRPC): Planned final analysis (FA) of COU-AA-301, a randomized, double-blind, placebo-controlled, phase III study of abiraterone acetate (AA) plus low-dose prednisone (P) post docetaxel. J Clin Oncol 2011;29:LBA4517.
38. Trerotola M, Li J, Alberti S, Languino LR. Trop-2 inhibits prostate cancer cell adhesion to fibronectin through the beta1 integrin-RACK1 axis. J Cell Physiol 2012;227:3670–7.
39. de Bono JS, Logothetis CJ, Molina A, Fizazi K, North S, Chu L, et al. Abiraterone and increased survival in metastatic prostate cancer. N Engl J Med 2011;364: 1995–2005.
40. Fizazi K, Scher HI, Molina A, Logothetis CJ, Chi KN, Jones RJ, et al. Abiraterone acetate for treatment of metastatic castration-resistant prostate cancer: final overall survival analysis of the COU-AA-301 randomised, double-blind, placebo-controlled phase 3 study. Lancet Oncol 2012;13: 983–92.
41. Rathkopf DE, Smith MR, de Bono JS, Logothetis CJ, Shore ND, de Souza P, et al. Updated interim efficacy analysis and long-term safety of abiraterone acetate in metastatic castration-resistant prostate cancer patients without prior chemotherapy (COU-AA-302). Eur Urol 2014;66:815–25.
42. Scher HI, Fizazi K, Saad F, Taplin ME, Sternberg CN, Miller K, et al. Increased survival with enzalutamide in prostate cancer after chemotherapy. N Eng J Med 2012;367:1187–97.
43. Beer TM, Armstrong AJ, Rathkopf DE, Loriot Y, Sternberg CN, Higano CS, et al. Enzalutamide in metastatic prostate cancer before chemotherapy. N Engl J Med 2014;371:424–33.
44. Bardia A, Mayer IA, Diamond JR, Moroose RL, Isakoff SJ, Starodub AN, et al. Efficacy and safety of anti-trop-2 antibody–drug conjugate sacituzumab govitecan (IMMU-132) in heavily pretreated patients with metastatic triple-negative breast cancer. J Clin Oncol 2017;35:2141–8.
45. Gray JE, Heist RS, Starodub AN, Camidge DR, Kio EA, Masters GA, et al. Therapy of small-cell lung cancer (SCLC) with a topoisomerase-I-inhibiting antibody–drug conjugate (ADC) targeting trop-2, sacituzumab govitecan. Clin Cancer Res 2017;23:5711–9.
46. Bardia A, Mayer IA, Vahdat LT, Tolaney SM, Isakoff SJ, Diamond JR, et al. Sacituzumab govitecan-hziy in refractory metastatic triple-negative breast cancer. N Eng J Med 2019;380:741–51.
47. Coates JT, Sun S, Leshchiner I, Thimmiah N, Martin EE, McLoughlin D, et al. Parallel genomic alterations of antigen and payload targets mediate polyclonal acquired clinical resistance to sacituzumab govitecan in triple-negative breast cancer. Cancer Discov 2021;11:2436–45.
48. de Wit S, van Dalum G, Lenferink AT, Tibbe AG, Hiltermann TJ, Groen HJ, et al. The detection of EpCAM(+) and EpCAM(−) circulating tumor cells. Sci Rep 2015;5:12270.